Materials Transactions, Vol. 48, No. 1 (2007) pp. 84 to 87

RAPID PUBLICATION

Characterization of β' Precipitate Phase in Mg-2 at% Y Alloy Aged to Peak Hardness Condition by High-Angle Annular Detector Dark-Field Scanning Transmission Electron Microscopy (HAADF-STEM)

Masahiko Nishijima, Kunio Yubuta and Kenji Hiraga

Institute for Materials Research, Tohoku University, Sendai 980-8577, Japan

The β' phase precipitated in an Mg-2 at%Y ($Mg_{98}Y_2$) alloy aged to a peak hardness condition at 200°C for 336 h has been studied by high-angle annular detector dark-field scanning transmission electron microscopy (HAADF-STEM). The β' precipitates have an about 20 nm size and definite facets parallel to the (010) plane, and Y-enriched double atom planes parallel to the (010) plane grow long and sometimes individually along the [100] and [001] directions. This morphology of the β' precipitates in the $Mg_{98}Y_2$ alloy is remarkably different from that in an $Mg_{95}Gd_5$ alloy. [doi:10.2320/matertrans.48.84]

(Received September 29, 2006; Accepted November 20, 2006; Published December 25, 2006)

Keywords: *magnesium alloy, magnesium-rare earth alloy, magnesium-yttrium, Mg-Y, precipitate, high-angle annular detector dark-field scanning transmission electron microscopy*

1. Introduction

It is well known that magnesium-based alloys containing rare earth elements such as Y, Gd Nd, and Dy show remarkable precipitation hardening by aging of supersaturated solid solutions of these alloys at low temperatures of about 200°C.[1–5] Transmission electron microscopy (TEM) and electron diffraction analysis of these alloys have proposed that β'' phase at the early stage of aging and β' phase at a peak hardness are precipitated.[1,4–10] Recently, some of the authors have studied the β' phase precipitates in an $Mg_{95}Gd_5$ alloy aged to a peak hardness condition by HAADF-STEM observations, and have proposed a new structure model of the β' phase, which is formed by an ordered arrangement of Gd-atoms in an Mg h.c.p. structure.[11] Also, details of the morphology and structural changes of the β' precipitates has been elucidated.[12] The previous work has demonstrated that HAADF-STEM is a powerful method for investigating of morphology of fine coherent precipitates.

The purpose of the present work is to reveal the morphology of β' phase precipitates in an $Mg_{98}Y_2$ alloy aged to a peak hardness condition by HAADF-STEM, by paying attention to the comparison between the morphology of the β' phase precipitates in the $Mg_{98}Y_2$ and $Mg_{95}Gd_5$ alloys.

An $Mg_{98}Y_2$ alloy was prepared by melting Mg (99.9%) and Y (99.9%) metals by induction heating under an Ar gas in a carbon crucible. The alloy was homogenized at 500°C for 6 h and then quenched in water. The alloy was aged at 200°C for 336 h. TEM specimens were cut from the aged alloy, and thinned by mechanical polishing and finally by ion-milling. HAADF-STEM images were taken by a 300 kV electron microscope (JEM-3000F) equipped with a field emission gun in the scanning transmission electron microscope mode. In HAADF-STEM observations, a beam probe with a half width of about 0.2 nm was scanned on samples.

2. Experimental Results

Figures 1(a) and 1(b) are electron diffraction patterns of the $Mg_{98}Y_2$ alloy, taken with the incident beam parallel to the $[001]_m$ (a) and $[110]_m$ (b) directions of the Mg-matrix, and Fig. 1(c) shows an electron diffraction pattern of an $Mg_{95}Gd_5$ alloy annealed at 200°C for 100 h for comparison. Extra diffraction spots in Fig. 1(a) result from three different variants around the $[001]_m$ axis, and the diffraction patterns show that the β' phase is coherently precipitated in the Mg-matrix. In Fig. 1(c), we can see the deformation from a face-centered rectangle arrangement of superlattice reflections of three variants around 1/2 0 0-typed positions, as can be seen by the comparison between arrangements of five superlattice spots in white circles in Figs. 1(a) and 1(c). The deformation suggests that lattice parameters of a- and b-axis for the orthorhombic β' phase are slightly different from $a = 2a_0$ and $b = 4\sqrt{3}a_0$. Lattice parameters of the orthorhombic β' phase were estimated as $a = 0.650$ nm, $b = 2.272$ nm and $c = 0.521$ nm in the $Mg_{95}Gd_5$ alloy aged at 250°C for 100 h.[12] As compared with $2a_0 = 0.6418$ nm, $4\sqrt{3}a_0 = 2.2232$ nm and $c_0 = 0.5210$ nm (a_0 and c_0 are lattice parameters of an Mg hexagonal lattice), there are remarkable differences for lattice parameters of a and b. On the other hand, superlattice reflections in Fig. 1(a) apparently form the face-centered rectangle arrangement, suggesting that lattice parameters of the orthorhombic β' phase in the $Mg_{98}Y_2$ alloy are $a = 2a_0 = 0.6418$ nm and $b = 4\sqrt{3}a_0 = 2.2232$ nm. Also, one can see superlattice reflections elongated along the a*-axis in Fig. 1(c),[12] whereas those in Fig. 1(a, b) are relatively elongated along the b*-axis, as can be seen in Fig. 1(b). These characteristics of superlattice reflections in the $Mg_{98}Y_2$ and $Mg_{95}Gd_5$ alloys will be understood from different morphology of the β' phase precipitates in the $Mg_{98}Y_2$ and $Mg_{95}Gd_5$ alloys.

Figure 2 is HAADF-STEM images of the $Mg_{98}Y_2$ alloy, taken with the incident beam parallel to the $[001]_m$ (a, c) and $[110]_m$ (b, d) directions of the Mg-matrix. The HAADF-STEM technique, which forms images from only high-angle

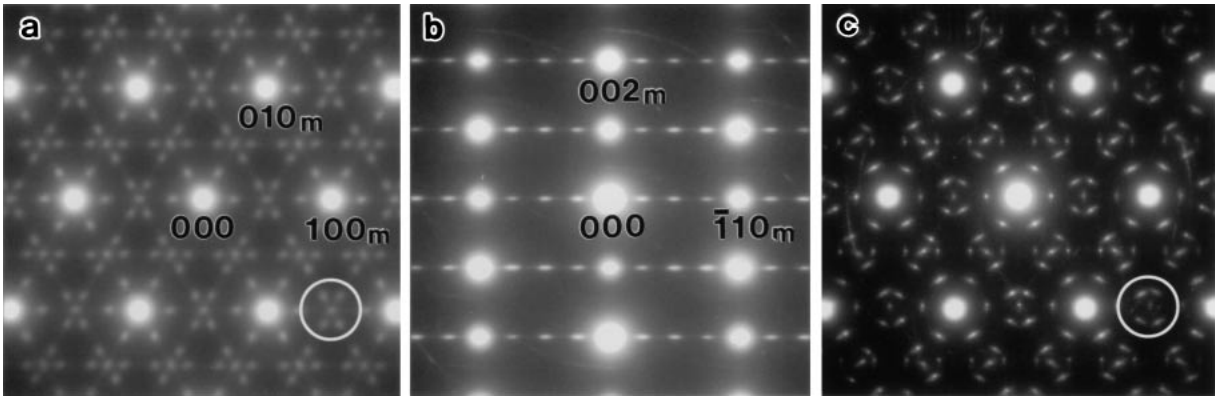

Fig. 1 Electron diffraction patterns of the $Mg_{98}Y_2$ alloy, taken with the incident beam parallel to the $[001]_m$ (a) and $[110]_m$ (b) directions of the Mg-matrix. (c) shows an electron diffraction pattern of the $Mg_{95}Gd_5$ alloy annealed at 200°C for 100 h, taken with the incident beam parallel to the $[001]_m$ of the Mg-matrix, for comparison. Diffraction spots are indexed by an Mg hexagonal structure. Note the remarkable deformation of an arrangement of five superlattice spots in a white circle in (c) from a face-centered rectangle arrangement of five spots in a white circle in (a).

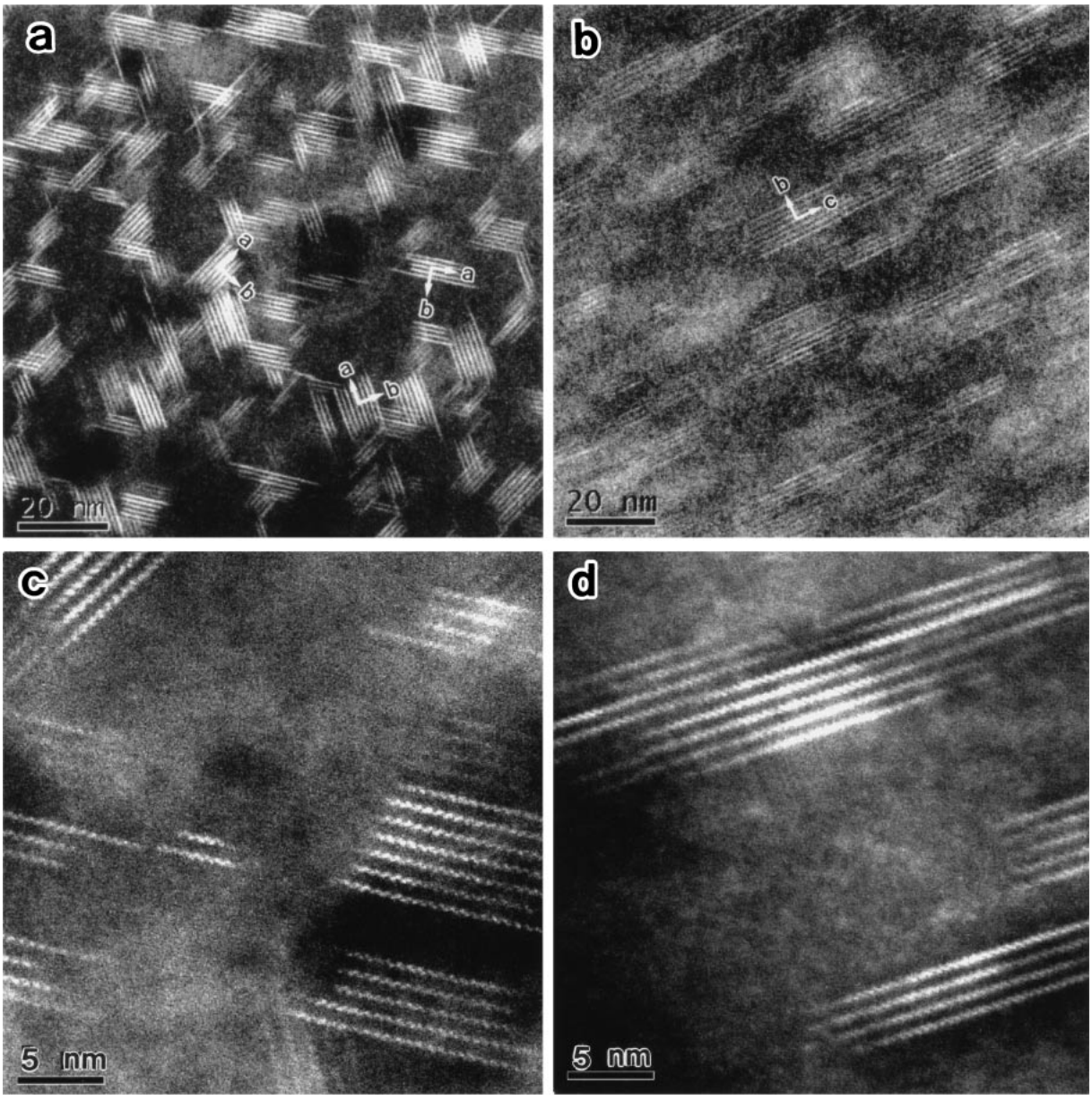

Fig. 2 HAADF-STEM images of the $Mg_{98}Y_2$ alloy, taken with the incident beam parallel to the $[001]_m$ (a, c) and $[110]_m$ (b, d) directions of the Mg-matrix. Primary axes of an orthorhombic structure of the β' phase are indicated by arrows.

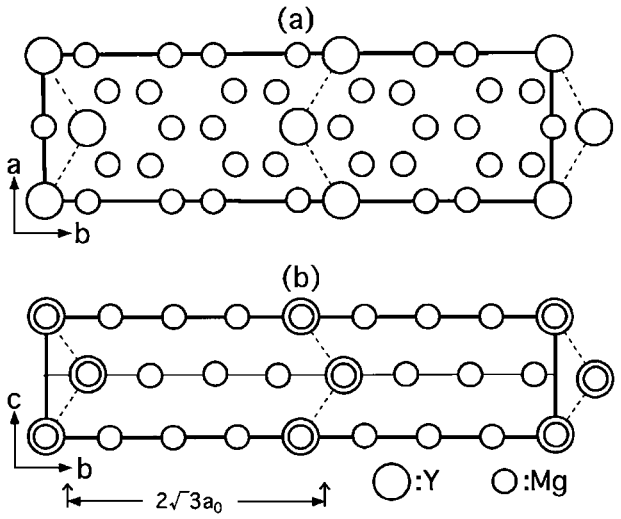

Fig. 3 An atomic arrangements of the Mg_7Y structure (β' phase), projected along the c-axis (a) and a-axis (b). A rectangle shows an orthorhombic unit cell. Note that zigzag arrays of Y atoms with an interval of $b/2 = 1.11$ nm, indicated by dotted lines, along the a- and c-axes in Y-enriched double atomic planes parallel to the (010) plane.

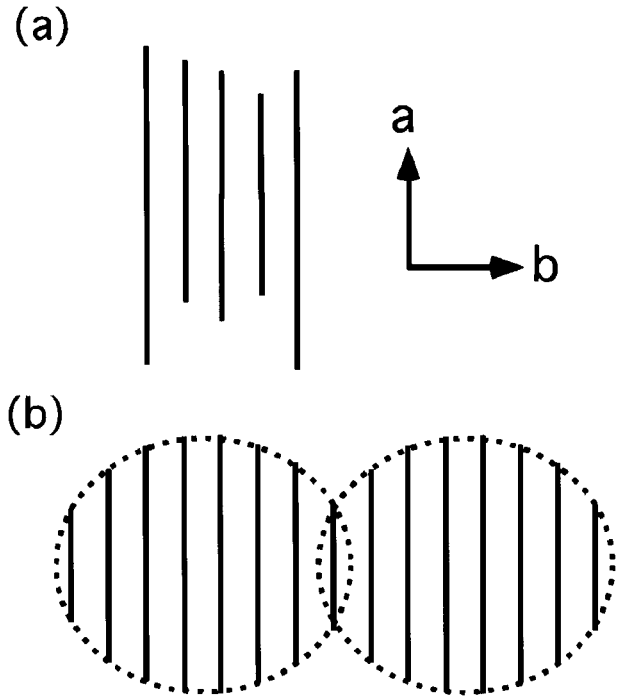

Fig. 4 Schematic illustrations showing the morphology of the β' precipitates in the top-aged $Mg_{98}Y_2$ (a) and $Mg_{95}Gd_5$ (b) alloys. Vertical thick lines correspond to the Y- or Gd-enriched double atomic planes in the structure of the β' phase.

scattered electrons, reproduces positions of heavy atoms and regions including heavy elements as bright contrast. Consequently, bright fringes with an interval of 1.1 nm in Fig. 2 can be concluded to be Y-enriched atomic planes. A structural model of the β' phase, which has been determined in an $Mg_{95}Gd_5$ alloy, is shown as atomic arrangements projected along the c-axis (a) and a-axis (b) in Fig. 3. In the Mg_7Y structure in Fig. 3, one can see zigzag arrays of Y atoms, indicated by dotted lines, in Y-enriched double planes parallel to the (010) plane. The zigzag arrays of Y atoms with an interval of $b/2 = 2\sqrt{3}a_0 = 1.11$ nm in the Mg_7Y structure can be seen in those of bright dots in Figs. 2(c) and 2(d).

Since the Y-enriched double planes are parallel to the (010) plane, bright fringes are always normal to the b-axis, which is parallel to $[210]_m$-typed directions of the Mg-hexagonal structure,[11] in Fig. 2. In Fig. 2(a), one can see three different variants of β' precipitates with different directions of a- and b-axes. In Fig. 2(b), precipitates with the a-axis parallel to the incident beam produce lattice fringes, and those without the a-axis parallel to the incident beam are represented as bright contrasts without lattice fringes. Surfaces normal to the b-axis in the precipitates have definite facets parallel to the (010) plane, but those normal to the a- and c-axis have no definite facets, and the independent growth of Y-enriched atomic planes along the a- and c-directions are often observed, as shown in a schematic illustration of Fig. 4(a). This morphology of the β' precipitates in the $Mg_{98}Y_2$ alloy is remarkably different from that of the β' precipitates in the $Mg_{95}Gd_5$ alloy aged to a peak hardness condition. The precipitates in the $Mg_{95}Gd_5$ alloy have definite shapes with an ellipse-like section in the a-b plane, as shown in a schematic illustration of Fig. 4(b), and the connection of precipitates along the b-axis forms planar-shaped precipitates.[11,12] The difference between morphology of the β' precipitates in the $Mg_{98}Y_2$ and $Mg_{95}Gd_5$ alloys is considered to be resulted from the difference between lattice parameters a and b for the Mg_7Gd and Mg_7Y structures. That is, lattice misfit between the β' precipitate and Mg-matrix in the $Mg_{95}Gd_5$ alloy forms minimum interfaces in the a-b plane, whereas no lattice misfit between the β' precipitate and Mg-matrix in the $Mg_{98}Y_2$ permits individual growth of Y-enriched atomic planes along the a- and c-directions.

Thin crystals of the β' precipitates in the $Mg_{95}Gd_5$ alloy along the a-axis, particularly at junction regions of the connection of precipitates, result in superlattice reflections elongated along the a*-axis in Fig. 1(c).[12] On the other hand, the β' precipitates in the $Mg_{98}Y_2$ alloy have thin crystals along the b-axis, compared with thicknesses along the b- and c-axes, and a few fringes along the b-axis are sometimes observed in Fig. 2. The thin precipitates along the b-axis in the $Mg_{98}Y_2$ alloy result in superlattice reflections relatively elongated along the b*-axis, as can be seen in Fig. 1(b).

3. Conclusion

HAADF-STEM observations of an $Mg_{98}Y_2$ alloy aged to a peak hardness condition give us much information about the morphology of β' phase precipitates. The precipitates have an about 20 nm size and definite facets parallel to the (010) plane, and Y-enriched double atom planes parallel to the (010) plane grow long along the [100] and [001] directions. This morphology of the β' precipitates in the $Mg_{98}Y_2$ alloy is remarkably different from that in an $Mg_{95}Gd_5$ alloy. The difference between morphology of the β' precipitates in the $Mg_{98}Y_2$ and $Mg_{95}Gd_5$ alloys is considered from the difference between lattice parameters of Mg_7Gd and Mg_7Y structures. That is, it is concluded that the difference between Mg_7Gd precipitates with relatively large lattice misfit and Mg_7Y ones with no misfit to the Mg-matrix lattice brings

about remarkably different morphology of β' precipitates in the $Mg_{98}Y_2$ and $Mg_{95}Gd_5$ alloys.

Acknowledgements

The authors are very grateful to Mr. T. Takahashi, Institute for Materials Research, Tohoku University, for preparing an $Mg_{98}Y_2$ alloy. This work is supported by the "Nanotechnology Support Project" of the Ministry of Education, Culture, Sports, Science and Technology (MEXT), Japan.

REFERENCES

1) L. L. Rokhlin: Phys. Met. Metall. **55** (1983) 98–103.
2) T. Sato, I. Takahashi, H. Tezuka and A. Kamio: Keikinzoku **42** (1992) 804–809.
3) S. Iwasawa, Y. Negishi, S. Kamado, Y. Kojima and R. Ninomiya: Keikinzoku **44** (1994) 3–8.
4) C. Antion, P. Donnadieu, F. Perrard, A. Deschamps, C. Tassin and A. Pisch: Acta Mater. **51** (2003) 5335–5348.
5) J. F. Nie, X. Gao and S. M. Zhu: Scripta Mater. **53** (2005) 1049–1053.
6) M. Hisa, J. C. Barry and G. L. Dunlop: *Proc. of the third International Magnesium Conf.* (The Institute of Materials, London, 1997) pp. 369–379.
7) S. Kamado, Y. Kojima, R. Ninomiya and K. Kubota: *Proc. of the third International Magnesium Conf.* (The Institute of Materials, London, 1997) pp. 327–342.
8) P. Vostrý, B. Smola, I. Strulíková, F. von Buch and B. L. Mordike: phy. stat. sol. (a) **175** (1999) 491–500.
9) B. Smola, I. Strulíková, F. von Buch and B. L. Mordike: Mater. Sci. and Eng. A **324** (2002) 113–117.
10) P. J. Apps, H. Karimzadeh, J. F. King and G. W. Lorimer: Scripta Mater. **48** (2003) 1023–1028.
11) M. Nishijima, K. Hiraga, M. Yamasaki and Y. Kawamura: Mater. Trans. **47** (2006) 2109–2112.
12) M. Nishijima and K. Hiraga: Mater. Trans. **48** (2007) 10–15.